Chapter 9
Dynamics of Vortices in Near-Wall Flows with Irregular Boundaries

I. M. Gorban and O. V. Khomenko

Abstract Behavior of stationary vortices in near-wall flows with irregular boundaries is investigated. The vortices were shown to locate in the critical points of flow and to be characterized not only by its strength but by the eigenfrequency that specifies precession of the vortex about the flow critical point along the small trajectory. Due to eigenfrequency, the stationary vortex responds selectively on external periodical perturbations. The last cause low-frequency vortex motion with large amplitudes and when the frequency of external perturbations is to be near the vortex eigenfrequency the vortex moves away from the critical point. So, dependency of the amplitude of perturbed vortex motion from the frequency of external perturbations has the resonance character. The resonant perturbations are shown to cause chaotization of local circulation zones generated by stationary vortices.

9.1 Introduction

Vortical structure of fluid flows is a determining factor when moving a body in water or in air as well as when operating hydraulic systems. A lot of important technical problems in fluid dynamics connect with optimal transformation of vortical pattern in the flow area. Artificial separation of flow resulting in generation of the local recirculation zone is the effective way that allows changing as the vortical flow pattern as the flow in whole. One may see the examples when artificial flow separation has been successfully applied in papers [1–6]. This method of control may be considered

I. M. Gorban (✉)
Institute of Hydromechanics, National Academy of Sciences of Ukraine,
8/4 Zheliabova St, Kyiv 03680, Ukraine
e-mail: ivgorban@gmail.com

O. V. Khomenko
Institute for Applied System Analysis, National Technical University of Ukraine
"Kyiv Polytechnic Institute", Peremogy ave., 37, build, 35, Kyiv03056, Ukraine
e-mail: olghomenko@mail.ru

as a way for regularization of near-wall flows at large Reynolds numbers. Transfer from a turbulent near-wall flow with chaotic motion of small-scale vortices to regular large-scale vortical pattern leads to reducing of energy exchange between the flow and the surface, in particular, to decreasing the body drag [3, 4]. The control strategy in this case is directed on creating the "intellectual" flow of fluid, in which the vortices are formed according to the control scheme and either theoretical or semiempirical model predicting the vortex behavior.

One of the ways to generate large-scale vortices in near-wall flow is artificial change of the surface configuration with help of bulges, grooves, ribs and so on [2–4]. The vortices may be immovable ones, stationary recirculation zones, or moving together with flow along the wall in regular manner. The fundamental requirement when generating the artificial vortex structures is their stability in respect of perturbations of external flow [7]. At the same time, the laboratory experiments testify fast response of the local separation zones to external perturbations, especially with a periodic component. This sensitivity is known to grow when rising the Reynolds number of flow. So, the progress in development of near-wall flow control algorithms connects with researching dynamical properties of the large-scale vortices and nature of their chaotic behavior.

Because of generation of large-scale vortices in near-wall flows is under action of viscous forces its investigation demands development of the mathematical models and numerical algorithms basing on the Navier-Stokes equations. At the same time, dynamical properties of the vortices, their stability and interaction with external flow may be studied within the scope of the model of ideal fluid. The efforts in investigation of the vortex dynamics have led to some understanding of chaotization of fluid flows [8–10].

It has to be noted that one of advantages of the vortex dynamic models, which don't take into consideration viscous effects, is their simplicity. This fact permits use these models for creation of algorithms of flow control in near-wall areas. Discovered recently properties of motion of vortices and fluid particles in near-wall flows have allowed to derive new ways of near-wall flow control [11–13].

It has been mentioned above one of the effective ways to change a near-wall flow pattern is installation of special irregularities on the wall, in particular, cross grooves. For the first time this method was proposed in papers [5–7] for decreasing hydraulic losses in diffusers. Developed by Ringleb [7] the model of standing vortices in the cross grooves of special configuration allowed derive new shapes of diffusers with minimal hydraulic losses. Use of the cross groove as a control element in aerodynamics was demonstrated in papers [3, 14] where an influence of shape, size and location of the groove on wing hydrodynamic characteristics was experimentally investigated.

At the same time, researches noted considerable instability of the flows with stationary recirculation zones and standing vortices [4, 15] that makes difficult its using in engineering. The knowledge about causes of this phenomenon would permit to broaden the practical application of the control schemes with standing vortices.

The analysis shows [15–17] that minimal energy losses for generating and supporting standing vortices will be achieved if one takes into account flow topology in

the region under consideration. Modern methods of near-flow control are connected with creating the needed flow topology that characterized by location of flow critical points, its type, separatrix shape and so on. Note the flow topology governs also chaotic processes in the region.

In the present paper, topology of the flows in the regions with non-regular boundaries and standing vortices is researched on the base of the standing vortex model. It will be shown that the vortex located in the neighborhood of a stable critical point is characterized by eigenfrequency which responsible for dynamical reaction of the vortex with external flow perturbations.

9.2 Model of Standing Vortex

A simplified model that describes dynamic properties of local recirculation zones formed near non-regular flow boundaries is considered. Linear parameters of the surface irregularity are supposed to exceed considerably the boundary layer thickness on the wall. The separation zone is simulated by a vortex that locates in the vorticity center and whose circulation is equal to integral vorticity strength in the region. In spite of simplicity, this model is effective enough for researching dynamic properties of near-wall flows [7].

Two-dimensional flow of ideal incompressible fluid bounded by non-regular wall is considered. Motion of a vortex located in this region is governed by a set of non-linear equations:

$$\frac{dx_v}{dt} = v_x(x_v, y_v, t), \quad \frac{dy_v}{dt} = v_y(x_v, y_v, t), \tag{9.1}$$

where x_v, y_v are the vortex coordinates and v_x, v_y are the components of the vortex velocity.

To determine the right part of system (9.1), one has to solve the Laplace equation for the complex flow potential Φ:

$$\Delta \Phi = 0 \tag{9.2}$$

with boundary conditions on the wall:

$$\left. \frac{\partial \Phi}{\partial n} \right|_{\Sigma} = 0, \tag{9.3}$$

and at infinity:

$$\left. \frac{\partial \Phi}{\partial z} \right|_{z \to \infty} = U_0, \tag{9.4}$$

Here Σ is the flow boundary and U_0 is the flow velocity.

Note if the velocity U_0 does not change in time, system (9.1) will be autonomous one. Analysis of its solutions may be carried out with applying the theory of critical points [18]. According to this theory, critical points of the flow with a vortex are determined from the condition of vortex equilibrium:

$$v_x(x_v, y_v) = 0, \quad v_y(x_v, y_v) = 0. \tag{9.5}$$

The divergence $divv = \dfrac{\partial v_x}{\partial x} + \dfrac{\partial v_y}{\partial y}$ and Jacobean $J = (\dfrac{\partial v_x}{\partial x})(\dfrac{\partial v_y}{\partial y}) - (\dfrac{\partial v_x}{\partial y})(\dfrac{\partial v_y}{\partial x})$ of set (9.1) specify the type of critical points. The critical point may be a saddle, if $J < 0$, a node, if $J < \pm\frac{div^2 v}{4}$, and a focus, if $J > \pm\frac{div^2 v}{4}$. Saddles are always unstable points, noses and foci may be either stable, when $divv < 0$, or unstable, when $divv > 0$. As we consider conservative flows, without energy supply, the divergence is equal to zero. Then critical points may be either unstable hyperbolic, if $J < 0$, or elliptical, when $J > 0$. For us, the latest points are interesting because they are conditionally stable ones and such a flow may be only realized in practice. The vortex, whose parameters are similar to those of the standing vortex, moves periodically around the elliptical point. For the standing vortex, the precession trajectory is infinitesimal and the precession frequency $\omega_0 = \sqrt{J}$ may be considered as its eigenfrequency. The eigenfrequency is a very important characteristic of the standing vortex. In particular, it governs the vortex reaction to external flow perturbations.

To find the solution of Eq. (9.2), we use the conformal mapping of the flow field in the physical z-plane into an upper half-plane of the auxiliary plane $\zeta(\xi, \eta)$. In ζ-plane, the complex flow potential is:

$$\Phi(\zeta) = \Phi_0(\zeta) + \frac{\Gamma}{2\pi i} \ln \frac{\zeta - \zeta_v}{\zeta - \overline{\zeta}_v}, \tag{9.6}$$

where Γ is the vortex circulation, ζ_v and $\Phi_0(\zeta)$ are the vortex complex coordinate and the non-separated flow potential in ζ-plane respectively.

If the conformal mapping function $\zeta = f(z)$ is known, one has the following expression for the vortex velocity in the physical plane:

$$\overline{v}(x_v, y_v) = \left(\frac{d\Phi_0}{d\zeta} + \frac{\Gamma}{4\pi\eta_v}\right) \frac{df}{dz}\bigg|_{\zeta=\zeta_v} + \frac{\Gamma}{4\pi i} \left(\frac{d^2 f}{dz^2} \bigg/ \frac{d\zeta}{dz}\right)\bigg|_{\zeta=\zeta_v}. \tag{9.7}$$

The real and imaginary components of (9.7) are the right-hand sides of (9.1).

The coordinates x_0, y_0 of the critical point are determined from the condition of the flow equilibrium here:

$$\overline{v}|_{z=z_0} = 0, \tag{9.8}$$

where $z_0 = x_0 + iy_0$.

Taking into account that coordinates of the critical point and the standing vortex coincide, we obtain from (9.7) the following equation:

$$\left(\frac{d\Phi_0}{d\zeta}\bigg|_{\zeta=\zeta_0} + \frac{\Gamma}{4\pi\eta_0}\right)\left[\left(\frac{df}{dz}\right)^2 \bigg/ \frac{d^2 f}{dz^2}\right]\bigg|_{\zeta=\zeta_0} - \frac{i\Gamma}{4\pi} = 0. \qquad (9.9)$$

From (9.9), two transcendental equations for determining the standing vortex coordinates are derived. To calculate the vortex circulation, this set has to be completed by an equation that follows from physical conditions of the problem under consideration. For example, if the flow boundary has a sharp edge, the unsteady Kutta condition can be involved.

9.3 Standing Vortex in Cross Groove

It was mentioned above cross grooves on the flowed surface are an effective way of near-wall flow control. We make here analysis of dynamic properties of the standing vortex in the uniform flow above the surface with a circular groove. The geometry of interest in the present study is presented in Fig. 9.1a. The mapping function that transforms the half-plane with a cut circular hollow (Fig. 9.1a) into the upper half-plane (Fig. 9.1b) has the following form:

$$f(z) = a\gamma\frac{1 + \left(\dfrac{z-a}{z+a}\right)^{\gamma}}{1 - \left(\dfrac{z-a}{z+a}\right)^{\gamma}}, \quad \gamma = \frac{\beta}{\pi - \beta} \qquad (9.10)$$

Here a is the semichord of groove, angle β characterizes the groove depth ($\beta < 0$). The dependence of the groove depth on the angle β is shown in Fig. 9.3, curve 1. The semichord a and the free-stream velocity U_0 are characteristic parameters of the problem. The dimensionless circulation is introduced as $\overline{\Gamma} = \Gamma/aU_0$.

The stationary point coordinates x_0, y_0 and standing vortex circulation Γ_0 are determined from (9.9) and Kutta condition in the sharp groove edges. The last requires finiteness of the flow velocity in the groove edge:
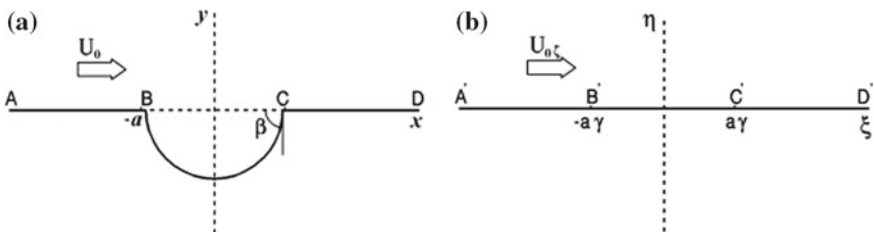
Fig. 9.1 Coordinate system in the physical plane z and the transformed plane ζ. Here $ABCD$ denote points in the physical plane which are mapped to points in the transformed plane $A'B'C'D'$

$$\frac{d\Phi}{dz}\bigg|_{z=z_*} = const, \tag{9.11}$$

where z_* is the coordinate of the sharp edge in the physical plane.

Using the ratio $\dfrac{d\Phi}{dz}\bigg|_{z=z_*} = \dfrac{d\Phi}{d\zeta}\dfrac{df}{dz}\bigg|_{z=z_*}$ and taking into account that the function $f(z)$ has a singularity in the sharp edge, one obtains:

$$\frac{d\Phi}{d\zeta}\bigg|_{\zeta=\zeta_*} = 0, \tag{9.12}$$

where $\zeta_*(\xi_*, 0)$ is the coordinate of the sharp edge in ζ-plane.

Taking into account symmetry of the flow region, it is sufficient to fulfill condition (9.12) in one groove edge only. As the unity flow in the physical plane transfers into the same flow in the transformed plane, from (9.6) the following equation may be derived:

$$\pi + \frac{\Gamma_0 \eta_0}{(\xi_* - \xi_0)^2 + \eta_0^2} = 0, \tag{9.13}$$

where (ξ_0, η_0) is the stationary point image in ζ-plane.

In the present research, Eqs. (9.9 and 9.13) are solved numerically with applying the secant method. The obtained results show that there are three stationary points when a vortex interacts with the stream in the considered region. As seen on the portrait of vortex trajectories (Fig. 9.2a), two points locate near the groove edges. As follows from analysis of their stability they are unstable. So, the flow with such standing vortices does not realize in physical experiment. The elliptical stationary point, which is conditionally stable, lies on the groove axis. The flow pattern corresponding such a standing vortex is shown in Fig. 9.2b.
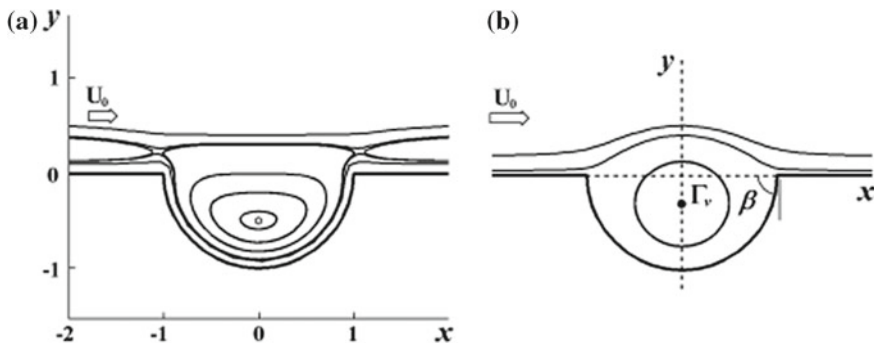
Fig. 9.2 Portrait of vortex trajectories—**a** and streamlines—**b** above the medium-sized groove ($\beta = -90°$)
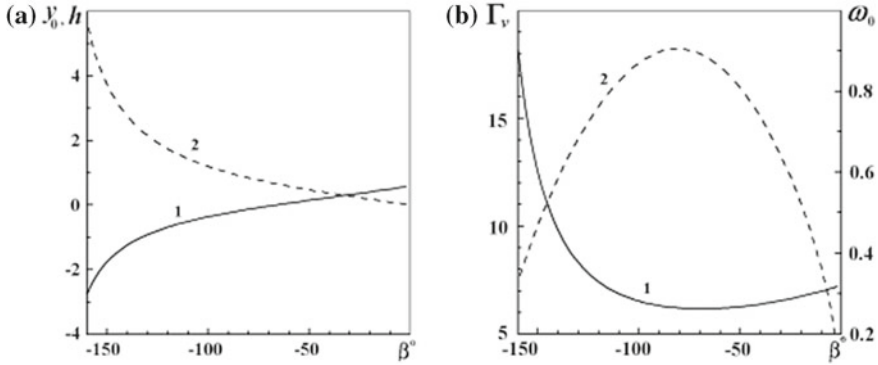
Fig. 9.3 Groove depth h (*curve 2*)—**a**, vertical coordinate y_0 (*curve 1*)—**a**, circulation Γ_v (*curve 1*)—**b** and eigenfrequency ω_0 (*curve 2*)—**b** of the standing vortex against the angle β

The vertical coordinate y_0 of the standing vortex against the angle β characterizing the groove depth is represented in Fig. 9.3a. It follows from this curve, the standing vortex locates above the wall for shallow grooves ($h < 0, 2$). So, a very small groove on the flowed surface promotes to stabilization of a vortex here. Because of the vortices placed above the flat wall are always non-stable, shallow grooves may be used for stabilization of vortices in near-wall flows. It is important for development of the control schemes that use stable vortices on the surface ("vortical lubrication" of a wall).

The circulation Γ_v and eigenfrequency ω_0 of standing vortex against the angle β are represented in Fig. 9.3b. These results point out fast reduction ω_0 as with increasing as with decreasing the groove depth. The standing vortex circulation Γ_v is large enough in deep hollows and it grows slightly in shallow grooves due to approaching the vortex to surface $y = 0$ in this case. Minimal circulation and maximal eigenfrequency of the standing vortex are observed in medium-sized hollows ($\beta \approx -90°$).

9.4 Standing Vortex in an Angular Region

In the simple cases, for example, when the fluid flow in an angular region is considered (Fig. 9.4), the standing vortex parameters may be obtained analytically. The following function maps interior of the angle β into a half-plane:

$$\zeta = z^{\frac{\pi}{\beta}}. \tag{9.14}$$

Taking into account that potential of irrotational flow is $\Phi_0(\zeta) = -\zeta$, one has motion equations of a vortex within the angular region in the following form:

Fig. 9.4 Flow pattern with the standing vortex in an angular region ($\beta = \frac{\pi}{2}$)
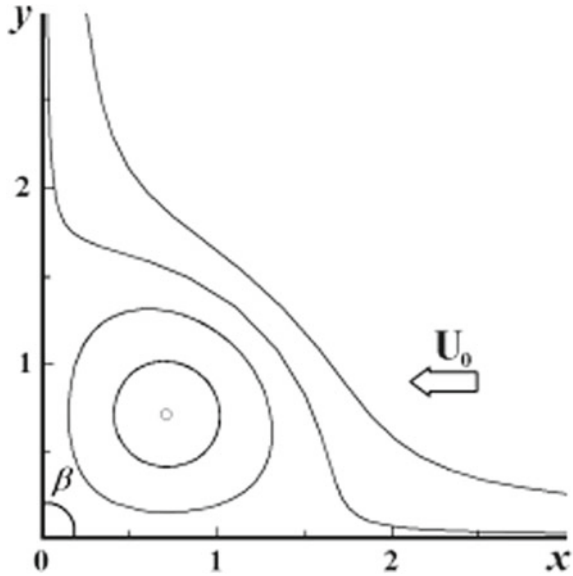
$$\frac{dx_v}{dt} = \left(\frac{\Gamma}{4\pi \sin \gamma \varphi} - 1\right) \gamma \cos \varphi(\gamma - 1) - \frac{\Gamma}{4\pi} y_v$$

$$\frac{dy_v}{dt} = -\left(\frac{\Gamma}{4\pi \sin \gamma \varphi} - 1\right) \gamma \sin \varphi(\gamma - 1) + \frac{\Gamma}{4\pi} x_v,$$

(9.15)

where $\varphi = \arctan \frac{y_v}{x_v}$, $\gamma = \frac{\pi}{\beta}$. The standing vortex circulation and coordinates of flow stationary point are derived by putting to zero the right-hand sides of (9.15):

$$\Gamma_0 = 4\pi\gamma, \quad x_0 = \cos \frac{\beta}{2}, \quad y_0 = \sin \frac{\beta}{2} \tag{9.16}$$

The carried out dynamic analysis shows the stationary point will be conditionally stable elliptic, when $\beta < \pi$. The circulation $\Gamma_v = \Gamma_0/4\pi$ and eigenfrequency ω_0 of the standing vortex against the angle β are represented in Fig. 9.5. Both the characteristics are seen growth when decreasing the angle β. So, the obtained results reveal the conditions when existence of the standing vortex in an angular region is possible and give value of the vortex parameters.

Fig. 9.5 The circulation Γ_v (*curve 1*) and eigenfrequency ω_0 (*curve 2*) of the standing vortex against angle β
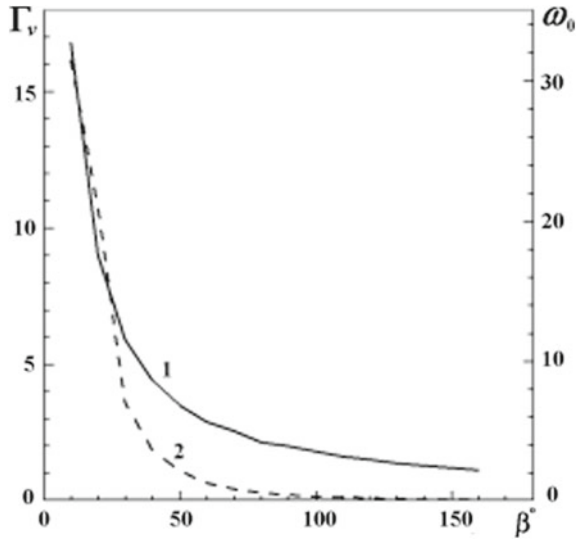
9.5 Resonant Properties of Standing Vortices and Their Behavior in Perturbed Flow

In practice, near-wall flows are heterogeneous. There are many factors that entail nonstationarity of an external stream, such as body vibrations, migration of turbulent spots and motion of external vortices. So, it is crucial to investigate how behavior of a standing vortex changes under external flow disturbances. We consider here periodic perturbations of the flow velocity:

$$U = U_0(1 + \varepsilon \sin \Omega t), \quad \varepsilon \ll 1 \tag{9.17}$$

where ε, Ω are the amplitude and frequency of perturbations respectively.

It is supposed that at an initial instance $t = 0$, the vortex of circulation Γ_0 locates in the stable stationary point (x_0, y_0). Reaction of the vortex on perturbations given by (9.17) will be studied. To determine the vortex trajectory in the perturbed flow, (9.1) are integrated numerically by a fourth-order Runge-Kutta method.

The obtained results show the standing vortex begins to move around its stationary position under influence of the external perturbations. Character of this motion depends on ratio between the external frequency Ω and the eigenfrequency ω_0. If the value of external frequency is far from that of eigenfrequency ω_0 or its subharmonics $\dfrac{\omega_0}{2}$ and $2\omega_0$, the vortex will move periodically on a closed trajectory in the small neighborhood of stationary point. The neighborhood size is proportional to the amplitude of perturbations ε. The vortex trajectory will be much more complicated

when the external frequency Ω tends to the vortex frequency ω_0 or its subharmonics. Then multiperiodic large amplitude motion of the standing vortex is generated.

Motion of the vortex is characterized by its deviation from the stationary point (x_0, y_0):

$$R(t) = \sqrt{(x_v(t) - x_0)^2 + (y_v(t) - y_0)^2}. \tag{9.18}$$

Then the maximum deviation

$$R_{max} = max\{R(t) \mid t = (0, \infty)\} \tag{9.19}$$

gives us the amplitude of vortex motion in the perturbed flow.

As follows from the results obtained, the amplitude R_{max} is finite although the external perturbation is small. It is due to non-linear character of the equations that govern motion of a vortex near complex flow boundaries. Dependence R_{max} on the perturbation frequency Ω has the resonant character. Under $\Omega \to \omega_0$, the amplitude of the vortex precession R_{max} increases rapidly.

The curves characterizing function $R_{max}\left(\dfrac{\Omega}{\omega_0}\right)$ in angular regions are depicted in Fig. 9.6. Three curves there correspond to different values β. These results approve the resonant character of interaction between the standing vortex and periodic perturbations of external flow. The sharpest display of that is observed for blunt angles.

Flow perturbations lead also to significant stimulation of fluid mixing in the recirculation zone. If perturbations are absent, fluid particles of this zone will move along closed trajectories around the standing vortex. Under resonant perturbation, advection of the fluid particles intensifies. To define the character of motion of fluid particles and of standing vortex in the perturbed flow, the corresponding Puincare

Fig. 9.6 Maximum deviation R_{max} of the standing vortex from the stationary point in an angular region against the relative frequency of external perturbation $\dfrac{\Omega}{\omega_0}$: $\varepsilon = 0, 01$, $1 - \beta = \dfrac{3\pi}{4}$, $2 - \beta = \dfrac{\pi}{2}$, $3 - \beta = \dfrac{\pi}{3}$.
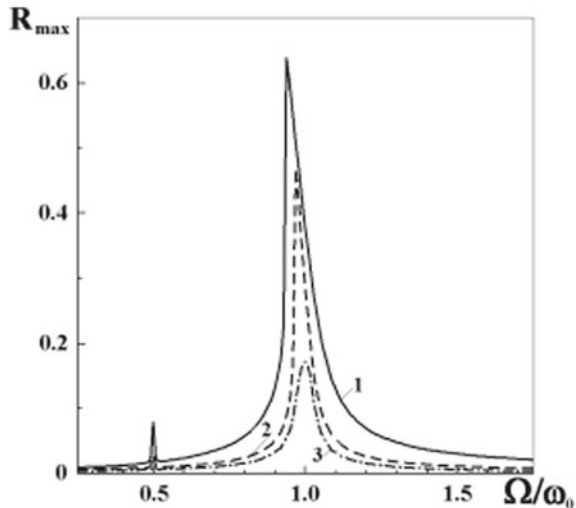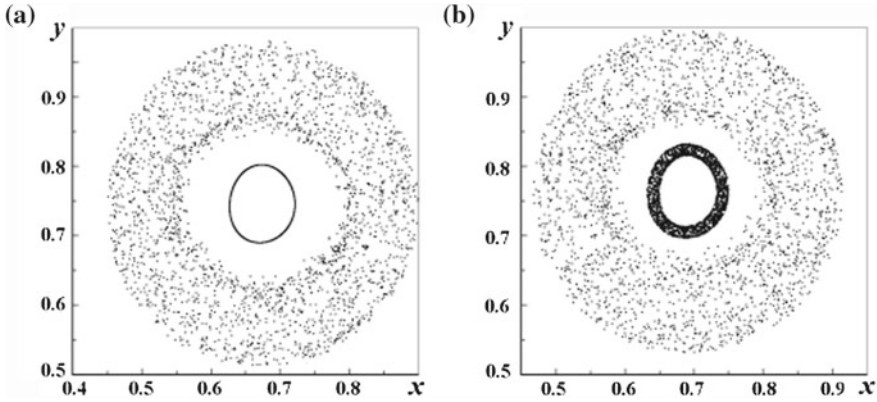
Fig. 9.7 Poincare sections of trajectories of the standing vortex and a fluid particle—**a** and two vortices of circulations $\Gamma_1 = \Gamma_v$ and $\Gamma_2 = \dfrac{\Gamma_v}{20}$—**b** in the angular region ($\beta = \dfrac{\pi}{2}$) at resonant flow perturbations: $\varepsilon = 0,001, \quad \Omega = \omega_0$

sections are computed when positions of particle or of vortex are calculated at the following points of time: $t_n = nT$, where $T = \dfrac{2\pi}{\Omega}$, $n = 1, 2, \dots$. Then those are plotted in the physical flow region. The resulting Puincare sections in the angular region with $\beta = \dfrac{\pi}{2}$ and $\Omega = \omega_0$, $\varepsilon = 0,01$ are represented in Fig. 9.7a. It denotes the chaotic motion of fluid particles because the points depicting the particle positions after the period fill closely certain area in the physical plane. On the contrary, the points corresponding to the vortex positions dispose along the closed curve that indicates on regular character of the vortex motion.

Figure 9.7b depicts Puincare sections for two vortices placed in the flow with resonant perturbations. One of those is the standing vortex of circulation Γ_v. At an initial instance, it is located in the stationary point (x_0, y_0). Another small vortex, whose circulation is $\dfrac{\Gamma_v}{20}$, moves around the first one. It is obvious that motion of the small vortex has chaotic character. But in this case, the standing vortex positions after the period fill the annulus of the finite thickness. It points out presence of secondary small vortices in the perturbed flow leads to chaotic motions of the large-scale vortex generated in the recirculation zone. Such dynamic reaction of the large vortex on the external perturbations is very important factor that acts on development of flow as a whole. Note it is an example of appearance of chaos in nonautonomous system.

The similar behavior of the standing vortex is observed in the periodically perturbed flow above the surface with a gross groove. Figure 9.8 demonstrates the vortex trajectory and corresponding time dependence of vortex deviation $R(t)$ from the stationary point under condition that the perturbation frequency Ω is close to the vortex eigenfrequency ω_0, ($\Omega = 1, 1\omega_0$). The vortex motion is likely to be multiperiodic one with a small basic frequency and high-frequency pulsations. The amplitude of the vortex oscillations R_{max} is comparable with the groove size. Note
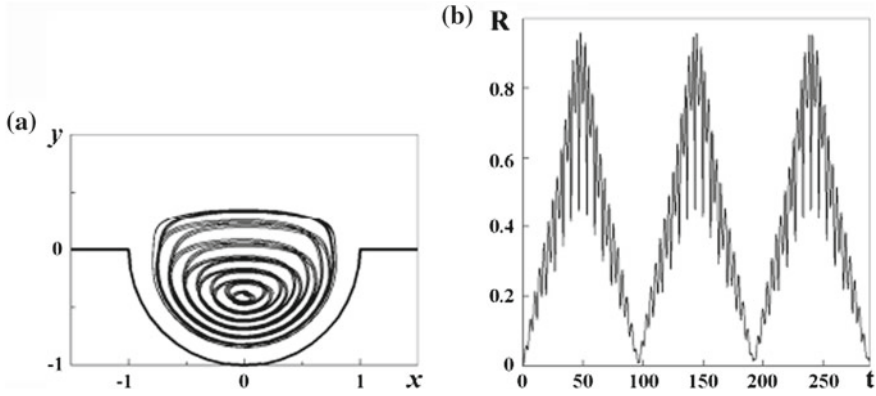
Fig. 9.8 Trajectory of the standing vortex in the perturbed flow near the wall with a groove—**a** and corresponding time dependence of the vortex deviation from the stationary point—**b**: $\varepsilon = 0, 1$, $\dfrac{\Omega}{\omega_0} = 1, 1$

Fig. 9.9 Trajectory of the standing vortex in the perturbed flow when the vortex is carried away from a groove: $\varepsilon = 0, 1$, $\dfrac{\Omega}{\omega_0} = 1, 15$
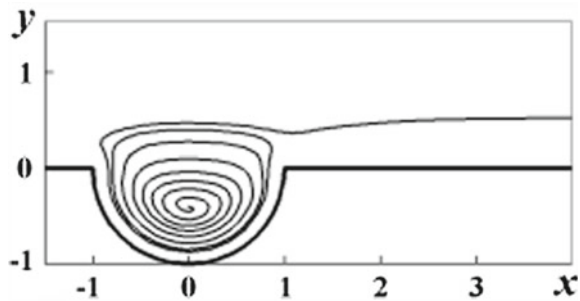
a Kutta-Joukowski condition satisfies in the sharp edges of the boundary as long as the vortex is in a small neighborhood of the stationary point. With increasing the amplitude of perturbed motion R_{max}, this condition violates and groove edges begin to generate vortex layers.

Other unfavorable outcome is connected with ejection of the vortex into the near-wall region that is possible when the perturbation amplitude grows (Fig. 9.9). From a standpoint of dynamic analysis, the vortex loses its stability and jumps across the separatrix between different trajectories on a phase portrait (Fig. 9.2). In practice, the vortex is carried away by flow. Taking into account continuous generation of vorticity in the upstream edge, one may predict periodical replication of this process that leads to degradation of body hydrodynamic characteristics.

Dependence of the amplitude of vortex perturbed motion R_{max} on relative frequency of external perturbation $\dfrac{\Omega}{\omega_0}$ has the resonant character (Figs. 9.10, 9.11). The size of resonant peak depends on both the amplitude of perturbation ε and the groove depth h (or angle β). Under $\varepsilon > 0, 1$, the secondary peaks of a resonant curve

Fig. 9.10 Maximum deviation R_{max} of the standing vortex from the stationary point in different grooves against the relative frequency of external perturbation $\dfrac{\Omega}{\omega_0}$:
$\varepsilon = 0,01,\quad 1 - \beta = -5°,$
$2 - \beta = -30°,\quad 3 - \beta = -150°$
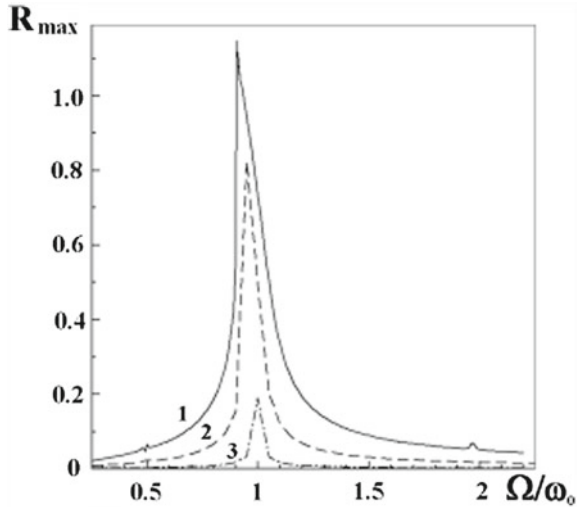
Fig. 9.11 Influence of intensity of external perturbations on dependence $R_{max}\left(\dfrac{\Omega}{\omega_0}\right)$:
$\beta = -\dfrac{\pi}{6},\quad 1 - \varepsilon = 0,02,\quad 2 - \varepsilon = 0,005$
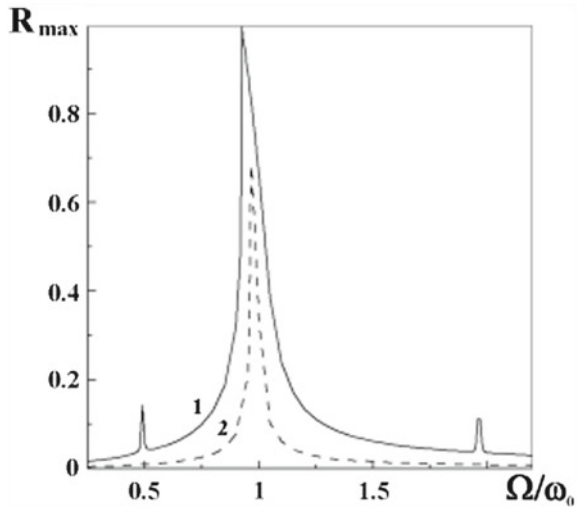
near the frequencies $\dfrac{\omega_0}{2}$ and $2\omega_0$ (Fig. 9.11) take place due to non-linear character of the considered dynamic system.

External periodic perturbations in the flow above a hollow also lead to chaotic motion of fluid particles and small vortices in the field governed by the standing vortex that intensifies fluid mixing.

The obtained results show that instability of the standing vortex generated in near-wall flow with a non-regular boundary is connected with periodic perturbations which are present in the free-stream. Response of the vortex to perturbation is maximal when

the perturbation frequency is close to the vortex eigenfrequency that is display of resonant interaction between the vortex and the perturbed flow.

9.6 Summary

The pattern of the near-wall flow bounded by a non-regular surface is shown to depend on flow topological properties, in particular, on a type of flow critical points and existing of stationary vortices. If the critical point is stable, a strong enough vortex may be generated in the point environment (standing vortex). The vortex stabilizes the near-wall flow due to suppression of vorticity generation in sharp edges of the boundary.

A standing vortex is characterized by its eigenfrequency which governs the dynamic behavior of the vortex in the periodically perturbed flow. Periodic oscillations of the flow velocity cause multiperiodic large amplitude motion of the standing vortex. The maximal amplitude of deviation of the vortex from its stationary point depends on the external perturbation frequency in resonance manner. When the perturbation frequency approaches to the vortex eigenfrequency, the deviation amplitude grows rapidly.

Resonance flow perturbations in the regions bounded non-regular wall cause intensification of fluid mixing in recirculation zones. They stimulate generation of vorticity in sharp boundary edges, lead to chaotization of motion of both fluid particles and small vortices, cause non-regular fluctuations of the flow.

The obtained results are useful for further development of control algorithms in near-wall flows as well as for understanding of chaotization processes in nonautonomous systems.

References

1. Belov, I.A.: Interaction of Nonuniform Flows with Obstacles. Mashinostroenie, Moskow (1983). (in Russian)
2. Chernyshenko, S.I., Galleti, B., Iollo, Z.L.: Trapped vortices and a favourable pressure gradient. J. Fluid. Mech. **482**, 235–255 (2003)
3. Mkhitaryan, A.M., Lukashuk, S.A., Trubenok, V.D., Fridland, V.Ya.: Influence of spoilers on the aerodynamic characteristics of a wing and a solid of revolution. Naukova Dumka, Kyiv, 254–263 (1966) (in Russian)
4. Zheng, P.: Flow Separation Control. Mir, Moskow (1979) (in Russian)
5. Migaj, V.K.: The aerodynamic efficiency of discontinuous surface. Eng. Phys. J. **4**, 20–23 (1962). (in Russian)
6. Migaj, V.K.: The study of a finned diffuser. Teploenergetika. **10**, 55–59 (1962). (in Russian)
7. Ringleb, F.O.: Two-dimensional flow with standing vortex in ducts and diffusers. Trans. ASME. J. Basic. Eng. **10**, 921–927 (1960)
8. Aref, H.: Integrable, chaotic and turbulent vortex motion in two-dimensional flows. Annu. Rev. Fluid. Mech. **15**, 345–389 (1983)

9. Aref, H., Kadtke, J.B., Zawadzki, I.: Point vortex dynamics: recent results and open problems. Fluid. Dyn. Res. **3**, 63–64 (1988)

10. Veretentsev, A.N., Geshev, P.I., Kuibin, P.A., Rudyak, V.Ya.: On the development of the method of vortex particles as applied to the description of detached flows. Zh. Vychisl. Mat. Mat. Fiz. **29**(6), 878–887 (1989) (in Russian)

11. Acton, E., Dhanak, M.R.: The motion and stability of a vortex above a pulsed surface. J. Fluid. Mech. **247**, 231–246 (1993)

12. Cortelezzi, L.: Nonlinear feedback control of the wake past a plate with a suction point on the downstream wall. J. Fluid. Mech. **327**, 303–324 (1996)

13. Cortelezzi, L., Leonard, A., Doyle, J.C.: An example of active circulation control of the unsteady separated flow past a semi-infinite plate. J. Fluid. Mech. **260**, 127–154 (1994)

14. Gorban, V., Gorban, I.: Dynamics of vortices in near-wall flows: eigenfrequencies, resonant properties, algorithms of control. AGARD. Rep. **827**, 1–11 (1998)

15. Gorban, V.O., Gorban, I.M.: Resonant properties of vortices at boundary irregularities. Rep. NAS. Ukraine. **2**, 44–47 (1996). (in Ukrainian)

16. Gorban, V.O., Gorban, I.M.: The Study of dynamics of the vortex structures in an angular area and near by surface with hollow. Appl. Hydromech. **1**(1), 4–11 (1999). (in Ukrainian)

17. Perry, A.E., Chong, M.S.: A description of eddying motion and flow patterns using critical-point concept. Annu. Rev. Fluid. Mech. **19**, 125–155 (1998)

18. Zaslavsky. G.M., Sagdeev R.Z.: Introduction to Nonlinear Physics. Nauka, Moskow (1988)